Hindawi Publishing Corporation
International Journal of Photoenergy
Volume 2014, Article ID 568185, 7 pages
http://dx.doi.org/10.1155/2014/568185

Research Article

Fe + N Noncompensated Codoping TiO_2 Nanowires: The Enhanced Visible Light Photocatalytic Properties

Zhongpo Zhou and Haiying Wang

The College of Physics and Electronic Engineering, Henan Normal University, Xinxiang 453007, Henan, China

Correspondence should be addressed to Haiying Wang; wanghaiy@whu.edu.cn

Received 9 March 2014; Accepted 17 March 2014; Published 7 April 2014

Academic Editor: Kangle Lv

The Fe + N codoped nanowire samples are prepared by hydro-thermal method and annealed in NH_3 atmosphere. The XRD (X-ray diffraction), SEM (Scanning electron microscope), UV-vis absorption spectroscopy, and BET (Brunauer, Emmett, and Teller) results indicate that the samples are pure anatase nanowires. The Fe + N codoped samples have the highest specific surface area, the largest red-shift, and the largest absorption enhancement in the visible light range compared with Fe doped, N doped, and undoped nanowires. The measurements of XPS (X-ray photoelectron spectroscopy) show that N content of Fe + N codoped TiO_2 is about two times as large as that of the N doped TiO_2. It is assumed that nitrogen doping plays a very important role for the photocatalytic activity increase and hence the Fe + N codoped nanowire TiO_2 shows the most effective photocatalytic activity under the visible light irradiation.

1. Introduction

Due to the strong photocatalytic activity, anti-photo-corrosion ability, biologic compatibility, and chemical stability of TiO_2, it has become the most promising photocatalysis [1–3]. However, the wide band gap of TiO_2 (3.2 eV for the anatase phase and 3.0 eV for the rutile phase) needs ultraviolet (UV) light for electron-hole separation, which is only 5% of the natural solar light [4]. It is of great significance to enlarge the TiO_2 absorption to visible light range and to improve the photocatalytic efficiency of it that can be used in visible light irradiation.

Recently, it was recognized that compared with metal ions (Ca^{2+}, Sr^{2+}, Ba^{2+}) [5], transition metal ions (Fe^{3+}, Cr^{6+}, Co^{3+}, Mo^{5+} [6–9]), rare earth cations (La^{3+}, Ce^{3+}, Er^{3+}, Pr^{3+}, Gd^{3+}, Nd^{3+}, Sm^{3+}) [10], and nonmetal doping (C [11, 12], S [13], F [14, 15], N [16, 17]), metal-nonmetal doped TiO_2 exhibited a valid process for narrowing the band gap and have been demonstrated to be more appropriate for extending the photocatalytic activity of TiO_2 into the visible region, such as Bi + C(N) codoping [18], Mo + C codoping [19], Mo + N codoping [20], Pr + N codoping [21], and Cd + N codoping [22]). As a result, it was found that the mon-odoping can generate the recombination center inside the TiO_2, which goes against the light-induced charge carriers' migration to the surface [19, 23]. In compensated n-type + p-type codopant systems, the defect bands can be passivated and will not be effective as carrier recombination centers [19, 24]. And the coulombic attraction between the n-type and p-type dopants with opposite charge substantially can enhance doping concentration of nonmetal [25]. Recently, noncompensated codoping was proposed by Romero-Gomez et al. [26], for its distinctive merit of ensuring the creation of intermediate electronic bands in the gap region and enhancing photoactivity manifested by efficient electron-hole separation in the visible-light region. Macak et al., Shankar et al., and Allam and El-Sayed pointed out that the morphology, crystallinity, composition, and illumination geometry of nanotube arrays were critical factors in their performance as photoelectrodes [27–29]. TiO_2 nanostructure materials displayed high performance for their potential in improving photocatalytic activity because of their high surface area.

In this work, the Fe + N noncompensated codoping nanowires are prepared by hydrothermal method and its

photocatalytic activities are evaluated by the degradation of methyl blue under visible light irradiation.

2. Experiments

Titanium isoproxide (Alfa Aesar company, 99.5%) was used as a starting material. Titanium foils (0.6 mm thick, 99.5% purity, cut in 1 × 2 cm^2) were prepared. Firstly, 10 mL titanium isoproxide solutions were dissolved in 62.5 mL absolute ethanol solutions. The solutions were then poured into 625 mL de-ionized water and stirred for 24 h. Then, ammonium hydroxide solution was added dropwise to keep the solution's pH value at 8. Then, the white gel precipitates were formed. The precipitates were collected by centrifuge and dried in an oven at 50°C for 24 h. Then the obtained powder was put into a Teflon bottle with a titanium foils at the bottom. The bottle was filled with 10 M NaOH and reacted at 180°C for 24 h. When the reaction was completed, the samples were purified by 0.1 M HNO_3 to remove the sodium ions. Finally, the samples were dried in an oven at 50°C for 12 h. The nitrogen-doped samples were obtained by annealing the samples in an ammonia atmosphere at 500°C for 2 h. For preparing the Fe-doped samples, firstly, 36 mg of iron nitrate hydrate was added into de-ionized water to obtain a doping concentration of 1 mol% in TiO_2. Then, the solution of iron nitrate hydrate and the solution of titanium isoproxide were dissolved in absolute ethanol and stirred for 24 h. Following the same procedure as that for pure samples and N doped samples, we can get Fe doped and Fe + N codoped samples. X-ray diffraction (XRD) patterns were collected on a Bruker AXS D8 Advance diffraction using the Cu K_a radiation at room temperature. The morphologies were recorded by scanning electron microscopy (SEM, FEI Sirion Field Emission Gun). X-ray photoelectron spectroscopy (XPS) with Mg Ka radiation was applied to investigate the surface composition and modifications on the chemical valence of the doping ions. The UV-visible absorption spectra were measured using a Cary 5000 UV-Vis-NIR spectrophotometer; $BaSO_4$ was used as a reflectance standard in a UV-visible diffuse reflectance experiment. The BET spectra were measured by specific surface area analyzer (V-sorb 2800P).

The photocatalytic activities under the visible light irradiation were evaluated by the degradation of methyl blue irradiated by a 450 W xenon lamp. In the process, the TiO_2 nanowire powder was immersed into a quartz colorimetric cuvette filled with 120 mL 10 mg/L methylene blue (MB) solution and placed below xenon lamp. The distance between the solution and the lamp was 10 cm distance. And the intensity of the light incident on the samples was about 900 mW/cm^2. The solution in the photoreactor was placed in the dark for 30 minutes to reach the absorption-desorption equilibrium.

3. Results and Discussion

Figure 1 shows the XRD patterns of Fe + N codoped, Fe doped, and undoped TiO_2 nanowires. As it can be seen from Figure 1, for all the samples, there are nine characteristic

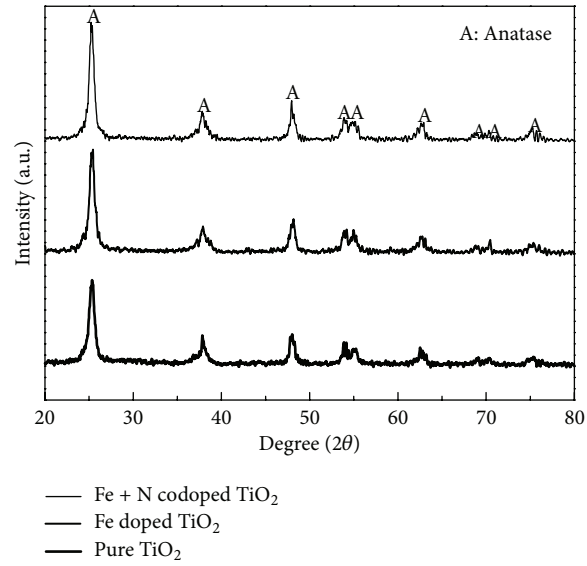

Figure 1: XRD patterns of Fe + N codoped, Fe doped, and undoped TiO_2 nanowires.

Table 1: Lattice constants, volume of the unit cell, and average crystallite sizes.

Sample	α (nm)	c (nm)	Volume (nm^3)
Undoped	0.3781	0.9510	0.1360
Fe doped	0.3775	0.9486	0.1352
Fe + N codoped	0.3782	0.9512	0.1362

diffraction peaks that appear at 25.36°, 37.88°, 47.99°, 53.93°, 55.06°, 62.69°, 68.80°, 70.32°, and 75.10°, which are in well accordance with the (101), (004), (200), (105), (211), (204), (116), (220), and (215) diffraction peak positions of anatase TiO_2 [JCP2.2CA: 21-1272]. No peaks of impurities (such as rutile, $FeTiO_3$, or Fe cluster) are detected. That is to say that all the samples are pure anatase phase. According to the Bragg equation, with a binary line regression fitting [30] using the (101), (004), (200), (105), and (211) characteristic peaks, the lattice constants a and c and the lattice volumes are estimated and listed in Table 1. It can be seen that, for Fe doped samples, the lattice constants a and c are smaller than that of the undoped samples, in accordance with that reported by Van Minh et al. [31]. As it is known that the atomic radius of Fe^{3+} (0.069 nm) is smaller than that of Ti^{4+} (0.075 nm), so after Fe^{3+} doping into Ti^{4+} site, the cell parameter will decrease. While for the Fe + N codoped samples, the lattice constants α and c are almost the same with the undoped samples.

SEM images of pure and Fe + N codoped TiO_2 samples are shown in Figure 2. It is found that for both samples, the shapes are nanowires and do not show any obvious change after the treatment in NH_3 flow at 500°C for 2 hours. The diameters of nanowires are about 50 nm and 40 nm for pure and Fe + N codoped TiO_2 samples, respectively. Obviously there is a little decrease in the diameter of Fe + N codoped nanowires, which is in accordance with the XRD results. The

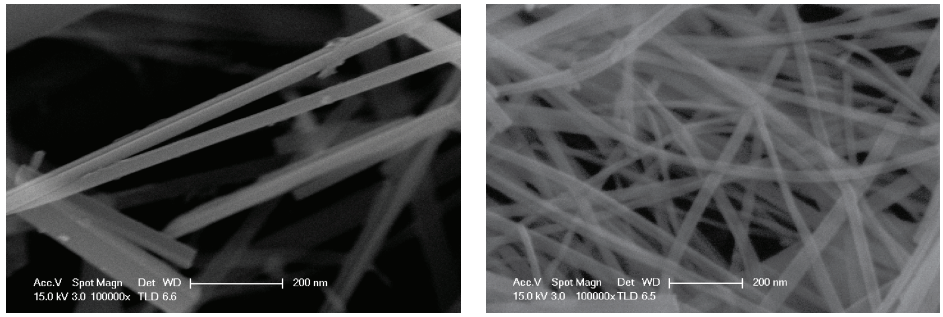

(a) (b)

Figure 2: SEM images of pure (a) and Fe + N codoped (b) TiO_2 nanowires.

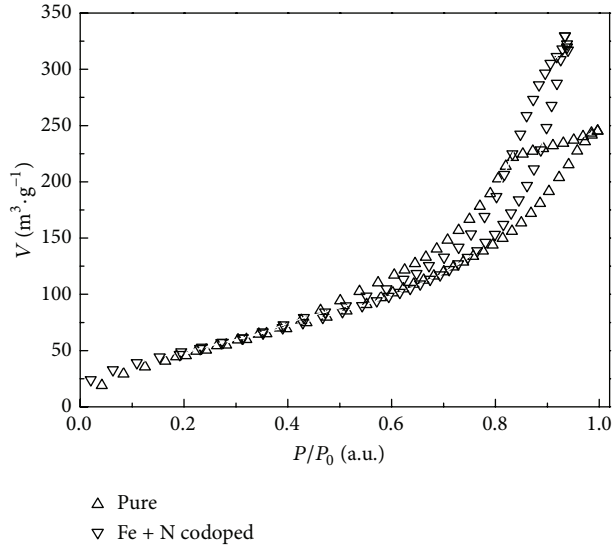

Figure 3: BET specific surface area of pure and Fe + N codoped TiO_2 nanowires.

doping of Fe and N elements may restrain the growth of nanowires, which is similar to the report in papers [32, 33].

The specific surface area is a macroscopic parameter which can be helpful to adjust the photocatalytic activity of photocatalyst. The specific surface areas gained from BET experiment measurements are 141.04 m^3/g, 145.151 m^3/g, 151.82 m^3/g, and 153 m^3/g for undoped, Fe doped, N doped, and Fe + N codoped TiO_2 nanowires, respectively. The specific surface area spectra of pure and Fe + N codoped TiO_2 nanowires are shown in Figure 3. It is believed that the specific surface area increase for Fe + N codoped TiO_2 nanowires comes from the decreased diameter size compared with undoped samples, as it can be seen from the SEM results.

In order to get the chemical states and the composition information, XPS measurements of Fe + N codoped nanowires were performed and the results are shown in Figure 4. Figure 4(a) shows the XPS survey spectrum of Fe + N codoped nanowires, where the peaks at 458.15, 530.67, 710.90, and 396.02 eV correspond to the binding energy of Ti $2p_{3/2}$, O 1s, Fe $2p_{3/2,}$ and N 1s, respectively. The C 1s peak observed at 284.71 eV is a signal of adventitious elemental carbon. There are no other impurity element observed in Figure 4(a), which confirms the existence of N element and Fe element in the Fe + N codoped samples lattices within the limits of instrumental error. The Fe 2p core level XPS spectrum of Fe + N codoped nanowires is showed in Figure 4(b). As we can see, there are two XPS peaks locating at 710.466 eV and 723.612 eV, close to the binding energy of the core level for Fe $2p_{3/2}$ and Fe $2p_{1/2}$ of Fe^{3+} ion, respectively [34]. The result provides the direct evidence for the conclusion that the valence of Fe ion is +3, occupies the Ti^{4+} site, and induces the cell parameter decrease. The calculation result by the Fe 2p core level spectrum shows that Fe content is 1.03%. Figure 4(c) shows the N 1s core level XPS spectra of N doped and Fe + N codoped nanowires. For N doped samples, there is one peak at the binding energy of 400.17 eV (labeled as N_B), while for Fe + N codoped samples, there are two peaks with similar intensity at the bonding energies of 396.02 eV and 400.17 eV (labeled as N_A and N_B), respectively, which is also reported by Drera et al. [35]. Normally, the peak position of N_B (at about 396 eV) reflects the formation of N–Ti–O bonds, indicating the substitution of N ions for O ions [36–38]. The peak position of N_B (at about 400 eV) can be assigned to molecular nitrogen bonded to surface defects or the N atoms bonding to O sites in TiO_2, forming Ti–O–N bonds. It is noticed that a new XPS peak (N_B peak) appears for Fe + N codoped samples compared with N doped samples, the larger N 1s peak area of Fe + N codoped samples may indicate that Fe + N codoping can enhance the N doping content on substituting sites. To confirm the suggestion, the N content is calculated from the N 1s core level spectra. The results show that the N contents are 1.87 mol% and 3.93 mol% for N-doped and Fe + N codoped samples. It verifies that codoping N with Fe increases the solubility of N in TiO_2, as reported in another paper [39].

Figure 5(a) illustrates the UV-vis absorption spectroscopy of the pure, Fe doped, N doped, and Fe + N codoped TiO_2 samples. The pure TiO_2 nanowire exhibits the characteristic spectrum of TiO_2 with its fundamental absorption sharp edge around 380 nm (3.2 eV band gap). Compared with the pure samples, the absorption edge of Fe doped, N doped, and Fe + N codoped samples is shifted towards visible light range and the absorptions significantly enhance in visible

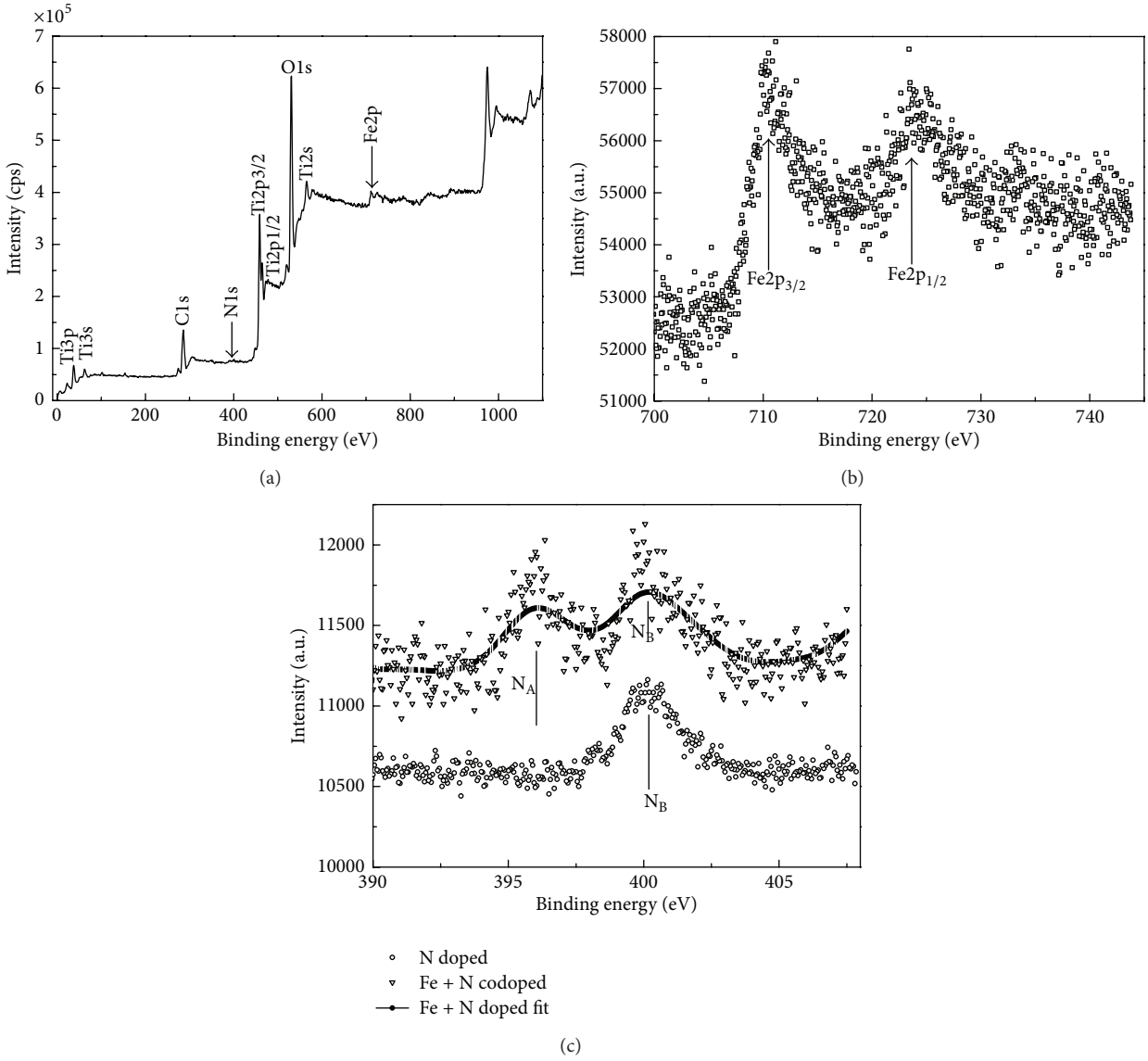

FIGURE 4: XPS spectra of (a) survey spectrum for Fe + N codoped TiO_2, (b) Fe 2p for Fe + N codoped TiO_2, and (c) N 1s for Fe + N codoped TiO_2 and the N-doped TiO_2.

light range. The spectrum of Fe + N codoped samples has the largest red-shift and the absorption enhancement in the visible light range. Figure 5(b) shows the plots of $(\alpha h\nu)^2$ versus $h\nu$ deduced from Figure 5(a). The band gap of each sample is determined by fitting the absorption spectra data according to the equation $(\alpha h\nu)^2 = B(h\nu - Eg)$ (α is the absorption coefficient; $h\nu$ is the photo energy; B is a constant number; and E_g is the absorption band gap energy). As it can be seen that the band gaps are 3.21 eV, 3.05 eV, 3.03 eV, and 3.02 eV of the pure, Fe doped, N doped, and Fe + N codoped TiO_2, respectively, which are similar to those reported in [40, 41], but much higher than the values calculated by Romero-Gomez et al. [26]. In this work, the contents of Fe element are about 1% for Fe doped and Fe + N codoped samples, and the contents of N element are about 1.87 mol% and 3.93 mol% for N-doped and Fe + N codoped samples. The reason for this deviation may be the lower doping content of N ions and Fe ions in experiments compared with the theoretical model.

As to the origin of the visible-light sensitivity by Fe doping, N doping, and Fe + N codoping, the possible mechanism can be put forward, similar with our previous work in [42]. It is known that doping with some nonmetal or metal elements in TiO_2 would tailor the band gap. Herein, for the Fe doping, the absorption edge red-shift could be understood by the band gap narrowing, which is the result of the induced sub-band-gap transition corresponding to the excitation of 3d electrons of Fe^{3+} to TiO_2 conduction band [41, 43]. For N doping, the doped N ions could induce an add-on shoulder on the edge of the valence band maximum and the localized N 2p states above the valence band [40]. At the

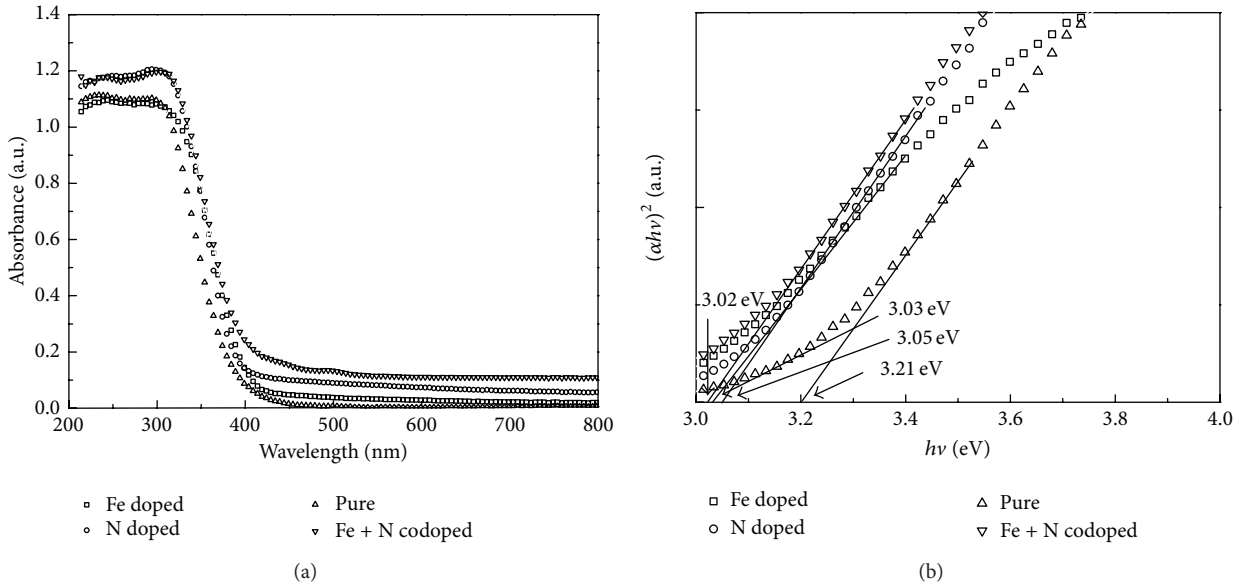

Figure 5: UV-vis absorption spectroscopy of pure, Fe doped, N doped, and Fe + N codoped TiO_2 with the wavelength in the range of (a) 200–800 nm and (b) $(\alpha h\nu)^2$ versus $h\nu$ curves.

same time, it is known that the valence state of N is lower than that of O so that the incorporation of N must promote the synchronous formation of oxygen vacancies for the charge equilibrium in TiO_2 [44]. Therefore, after N doping the band gap narrows resulting in the newly formed oxygen vacancies in TiO_2 lattices which cannot be neglected. As a result, after N doping, the visible light response is attributed to both oxygen vacancies and the N 2p states. For Fe + N codoping, after N ions dope into the TiO_2 lattices, the Fe ions are introduced into the lattice of TiO_2 as the oxidation state of Fe^{3+} confirmed by the XPS results. Here Fe-doping is a p-type doping and it can increase the oxygen vacancies induced by the holes doping of N, similar to [44]. Consequently, the codoped TiO_2 results in the best response to visible-light and the largest red-shift because of the synergistic effect of Fe ions and N ions codoping.

The MB degradation experiments were carried out in an aqueous solution under visible light irradiation by inserting a filter ($\lambda \leq 400$ nm) between the Xe-lamp and the samples. Figure 6 shows the photocatalytic degradation curves of MB catalyzed by the samples. The photocatalytic activity is in the order of the Fe + N codoped TiO_2 > N-doped TiO_2 > Fe-doped TiO_2 > undoped TiO_2. The Fe + N codoped TiO_2 nanowires exhibit the best photocatalytic activity, and the removal of MB is about 59% after 4 hours of irradiation under visible light. For nitrogen doped samples, density functional theory (DFT) calculations [45] have shown a large decrease in the formation energy for oxygen vacancies as a result of the presence of nitrogen atoms in the lattice and the neglected band narrowing is seen. While for Fe + N codoped samples, compared with the N doped TiO_2, Fe-doping is a p-type doping and it can increase the oxygen vacancies induced by the hole doping of N, similar to [44]. It has been reported that oxygen vacancies induced by N-doping, Fe-doping, or self-doping play an important role in the photocatalytic activity of TiO_2 nanowires by trapping the photoinduced electron and acting as a reactive center for the photocatalytic process [46, 47]. As a result, the Fe + N codoped nanowires gain the best visible-light response. At the same time, after Fe + N codoping the Fe + N codoped nanowires yield the highest specific surface area. Therefore, it is not surprising that the Fe + N codoped nanowires show the best photocatalytic activity by visible light irradiation.

4. Conclusions

The Fe + N codoped nanowire samples are prepared by hydrothermal method in 10 M NaOH and annealed in NH_3 atmosphere at 500°C. The XRD and SEM results show that the Fe + N codoped samples are pure anatase nanowires with 40 nm diameter, which is smaller than the pure TiO_2 nanowires whose average diameter is about 50 nm. The UV-vis absorption spectroscopy and BET results indicate the highest specific surface area, the largest red-shift, and the largest absorption enhancement in the Fe + N codoped nanowires compared with that in Fe doped, N doped, and undoped nanowires in visible light range. The measurements of XPS show that the N doped samples have the N content of 1.87 mol%, while Fe + N codoped TiO_2 have the N content of 3.93 mol%, which is about two times as large as that of the N doped TiO_2. It was assumed that the iron and N codoping can rapidly increase the N content in TiO_2. Hence, the Fe + N codoped nanowires show the most effective photocatalytic activity under visible light irradiation for doubled N content and the synergistic effects of codoped nitrogen and iron ions.

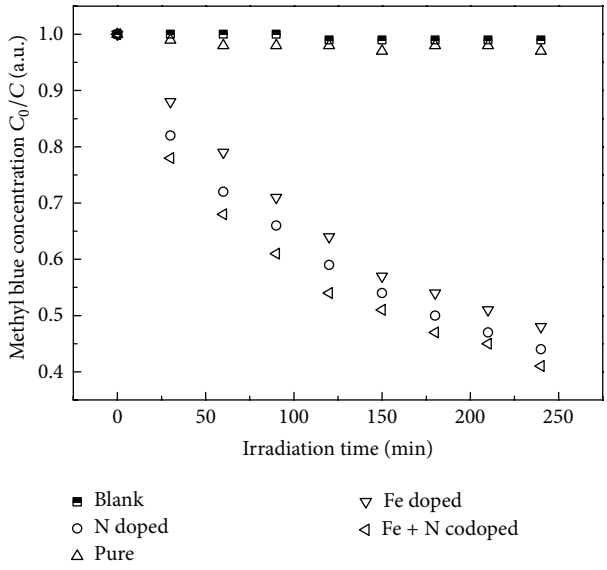

Figure 6: Concentrations of methyl blue photo-degraded by the pure, N doped, Fe doped, and Fe + N codoped TiO_2.

Conflict of Interests

The authors declare that there is no conflict of interests regarding the publication of this paper.

Acknowledgments

This work is supported by the CPSF under Grant no. 01026500204, the NSFC under Grant no. 11304083, and the Scientific Research Foundation for PHD of Henan Normal University under Grant nos. 01026500257 and 01026500121.

References

[1] A. Fujishima and K. Honda, "Electrochemical photolysis of water at a semiconductor electrode," *Nature*, vol. 238, no. 5358, pp. 37–38, 1972.

[2] S. Sreekantan, R. Hazan, and Z. Lockman, "Photoactivity of anatase-rutile TiO_2 nanotubes formed by anodization method," *Thin Solid Films*, vol. 518, no. 1, pp. 16–21, 2009.

[3] A. Fujishima, T. N. Rao, and D. A. Tryk, "Titanium dioxide photocatalysis," *Journal of Photochemistry and Photobiology C*, vol. 1, no. 1, pp. 1–21, 2000.

[4] X. B. Chen and S. S. Mao, "Titanium dioxide nanomaterials: synthesis, properties, modifications, and applications," *Chemical Reviews*, vol. 107, no. 7, pp. 2891–2959, 2007.

[5] N. I. Al-Salim, S. A. Bagshaw, A. Bittar et al., "Characterisation and activity of sol-gel-prepared TiO_2 photocatalysts modified with Ca, Sr or Ba ion additives," *Journal of Materials Chemistry*, vol. 10, no. 10, pp. 2358–2363, 2000.

[6] M. Kang, "Synthesis of Fe/TiO_2 photocatalyst with nanometer size by solvothermal method and the effect of H_2O addition on structural stability and photodecomposition of methanol," *Journal of Molecular Catalysis A: Chemical*, vol. 197, no. 1-2, pp. 173–183, 2003.

[7] K. Wilke and H. D. Breuer, "The influence of transition metal doping on the physical and photocatalytic properties of titania," *Journal of Photochemistry and Photobiology A: Chemistry*, vol. 121, no. 1, pp. 49–53, 1999.

[8] J. Wang, S. Uma, and K. J. Klabunde, "Visible light photocatalysis in transition metal incorporated titania-silica aerogels," *Applied Catalysis B: Environmental*, vol. 48, no. 2, pp. 151–154, 2004.

[9] Y. Yang, X. J. Li, J. T. Chen, and L. Y. Wang, "Effect of doping mode on the photocatalytic activities of Mo/TiO_2," *Journal of Photochemistry and Photobiology A: Chemistry*, vol. 163, no. 3, pp. 517–522, 2004.

[10] A. W. Xu, Y. Gao, and H. Q. Liu, "The Preparation, characterization, and their photocatalytic activities of rare-earth-doped TiO_2 nanoparticles," *Journal of Catalysis*, vol. 207, no. 2, pp. 151–157, 2002.

[11] S. U. M. Khan, M. Al-Shahry, and W. B. Ingler Jr., "Efficient photochemical water splitting by a chemically modified n-TiO_2," *Science*, vol. 297, no. 5590, pp. 2243–2245, 2002.

[12] K. L. Lv, J. C. Hu, X. H. Li, and M. Li, "Cysteine modified anatase TiO_2 hollow microspheres with enhanced visible-light-driven photocatalytic activity," *Journal of Molecular Catalysis A: Chemical*, vol. 356, pp. 78–84, 2012.

[13] T. Umebayashi, T. Yamaki, H. Itoh, and K. Asai, "Band gap narrowing of titanium dioxide by sulfur doping," *Applied Physics Letters*, vol. 81, no. 3, pp. 454–456, 2002.

[14] T. Yamaki, T. Sumita, and S. Yamamoto, "Formation of $TiO_{2-x}F_x$ compounds in fluorine-implanted TiO_2," *Journal of Materials Science Letters* , vol. 21, no. 1, pp. 33–35, 2002.

[15] G. J. Ren, Y. Gao, X. Liu, A. Xing, H. T. Liu, and J. G. Yin, "Synthesis of high-activity F-doped TiO_2 photocatalyst via a simple one-step hydrothermal process," *Reaction Kinetics, Mechanisms and Catalysis*, vol. 100, pp. 487–497, 2010.

[16] L. Dong, G. X. Cao, Y. Ma, X. L. Jia, G. T. Ye, and S. K. Guan, "Enhanced photocatalytic degradation properties of nitrogen-doped titania nanotube arrays," *Transactions of Nonferrous Metals Society of China*, vol. 19, no. 6, pp. 1583–1587, 2009.

[17] H. Y. Wang, Y. C. Yang, J. H. Wei et al., "Effective photocatalytic properties of N doped Titanium dioxide nanotube arrays prepared by anodization," *Reaction Kinetics, Mechanisms and Catalysis*, vol. 106, pp. 341–353, 2012.

[18] K. L. Lv, H. S. Zuo, J. Sun et al., "(Bi, C and N) codoped TiO_2 nanoparticles," *Journal of Hazardous Materials*, vol. 161, no. 1, pp. 396–401, 2009.

[19] Y. Gai, J. Li, S. S. Li, J. B. Xia, and S. H. Wei, "Design of narrow-gap TiO_2: a passivated codoping approach for enhanced photoelectrochemical activity," *Physical Review Letters*, vol. 102, Article ID 036402, 2009.

[20] H. Liu, Z. Lu, and L. Yue, "(Mo + N) codoped TiO_2 for enhanced visible-light photoactivity," *Applied Surface Science*, vol. 257, no. 22, pp. 9355–9361, 2011.

[21] J. Yang, J. Dai, and J. Li, "Synthesis, characterization and degradation of Bisphenol A using Pr, N co-doped TiO_2 with highly visible light activity," *Applied Surface Science*, vol. 257, no. 21, pp. 8965–8973, 2011.

[22] H. Gao, B. Lu, F. Liu, Y. Liu, and X. Zhao, "Photocatalytical properties and theoretical analysis of N, Cd-codoped TiO_2 synthesized by thermal decomposition method," *International Journal of Photoenergy*, vol. 2012, Article ID 453018, 9 pages, 2012.

[23] T. Umebayashi, T. Yamaki, H. Itoh, and K. Asai, "Analysis of electronic structures of 3d transition metal-doped TiO_2 based on band calculations," *Journal of Physics and Chemistry of Solids*, vol. 63, no. 10, pp. 1909–1920, 2002.

[24] K. S. . Ahn, Y. Yan, S. Shet, T. Deutsch, J. Turner, and M. Al-Jassim, "Enhanced photoelectrochemical responses of ZnO films through Ga and N codoping ," *Applied Physics Letters*, vol. 91, no. 23, Article ID 231909, 2007.

[25] W. Zhu, X. Qiu, and V. Iancu, "Band gap narrowing of titanium oxide semiconductors by noncompensated anion-cation codoping for enhanced visible-light photoactivity," *Physical Review Letters*, vol. 103, Article ID 226401, 2009.

[26] P. Romero-Gomez, A. Borras, A. Barranco, J. P. Espinos, and A. R. Gonzalez-Elipe, "Enhanced photoactivity in bilayer films with buried rutile-anatase heterojunctions," *ChemPhysChem*, vol. 12, no. 1, pp. 191–196, 2011.

[27] J. M. Macak, H. Tsuchiya, A. Ghicov et al., "TiO_2 nanotubes: Self-organized electrochemical formation, properties and applications," *Current Opinion in Solid State and Materials Science*, vol. 11, no. 1-2, pp. 3–18, 2007.

[28] K. Shankar, J. I. Basham, N. K. Allam et al., "Recent advances In the use of TiO_2 nanotube and nanowire arrays for oxidative photoelectrochemistry," *Journal of Physical Chemistry C*, vol. 113, no. 16, pp. 6327–6359, 2009.

[29] N. K. Allam and M. A. El-Sayed, "Photoelectrochemical water oxidation characteristics of anodically fabricated TiO_2 nanotube arrays: structural and optical properties," *Journal of Physical Chemistry C*, vol. 114, no. 27, pp. 12024–12029, 2010.

[30] Y. T. Fei, *Error Theory and Data Processing*, China Machine Press, Beijing, China, 2006.

[31] N. Van Minh, D. H. Long, N. T. Khoi, Y. Jung, S. J. Kim, and I. S. Yang, "Raman studies of $Ti_{bm1-x}Fe_{bmx}O_{bm2}$ nanoparticles," *IEEE Transactions on Nanotechnology*, vol. 7, no. 2, pp. 177–180, 2008.

[32] J. Yu, M. Zhou, H. Yu, Q. Zhang, and Y. Yu, "Enhanced photoinduced super-hydrophilicity of the sol–gel-derived TiO_2 thin films by Fe-doping," *Materials Chemistry and Physics*, vol. 95, no. 2-3, pp. 193–196, 2006.

[33] W. Q. Peng, M. Yanagida, and L. Y. Han, "Rutile-anatase TiO_2 photoanodes for dye-sensitized solar cells," *Journal of Nonlinear Optical Physics & Materials*, vol. 19, no. 4, p. 673, 2010.

[34] C. D. Wagner, W. M. Riggs, L. E. Davis, J. F. Moulder, and G. E. Muilenberg, *Handbook of X-Ray Photoelectron Spectroscopy*, Perkin-Elmer Corporation, Physical Electronics Division, Eden Prairie, Minn, USA, 1979.

[35] G. Drera, M. C. Mozzati, P. Galinetto et al., "Response to "comment on 'Enhancement of room temperature ferromagnetism in N-doped TiO_{2-x} rutile: Correlation with the local electronic properties'" [Appl. Phys. Lett. 97, 186101 (2010)]," *Applied Physics Letters*, vol. 97, no. 18, Article ID 186102, 2010.

[36] C. S. Gopinath, "Comment on 'photoelectron spectroscopic investigation of nitrogen-doped titania nanoparticles'," *Journal of Physical Chemistry B*, vol. 110, no. 13, pp. 7079–7080, 2006.

[37] C. Burda and J. Gole, "Reply to 'comment on 'photoelectron spectroscopic investigation of nitrogen-doped titania nanoparticles'"," *Journal of Physical Chemistry B*, vol. 110, no. 13, pp. 7081–7082, 2006.

[38] J. F. Molder, W. F. Stickle, P. E. Sobol, and K. D. Bomben, *Handbook of X-Ray Photoelectron Spectroscopy*, Perkin-Elmer, Eden Prairie, Minn, USA, 2nd edition, 1992.

[39] H. Y. Wang, J. H. Wei, R. Xiong, and J. Shi, "Enhanced ferromagnetic properties of Fe+N codoped TiO_2 anatase," *Journal of Magnetism and Magnetic Materials*, vol. 324, no. 13, pp. 2057–2061, 2012.

[40] J. Yu, Q. Xiang, and M. Zhou, "Preparation, characterization and visible-light-driven photocatalytic activity of Fe-doped titania nanorods and first-principles study for electronic structures," *Applied Catalysis B: Environmental*, vol. 90, no. 3-4, pp. 595–602, 2009.

[41] W. Choi, A. Termin, and M. R. Hoffmann, "The role of metal ion dopants in quantum-sized TiO_2: correlation between photoreactivity and charge carrier recombination dynamics," *Journal of Physical Chemistry*, vol. 98, no. 51, pp. 13669–13679, 1994.

[42] K. W. Li, H. Y. Wang, C. X. Pan, P. F. Fang, R. Xiong, and J. Shi, "Enhanced photoactivity of Fe+N codoped anatase-rutile TiO_2 nanowire film under visible light irradiation," *International Journal of Photoenergy*, vol. 2012, Article ID 398508, 8 pages, 2012.

[43] K. Tan, H. Zhang, C. Xie, H. Zheng, Y. Gu, and W. F. Zhang, "Visible-light absorption and photocatalytic activity in molybdenum- and nitrogen-codoped TiO_2," *Catalysis Communications*, vol. 11, no. 5, pp. 531–335, 2010.

[44] T. Ihara, M. Miyoshi, Y. Iriyama, O. Matsumoto, and S. Sugihara, "Visible-light-active titanium oxide photocatalyst realized by an oxygen-deficient structure and by nitrogen doping," *Applied Catalysis B: Environmental*, vol. 42, no. 4, pp. 403–409, 2003.

[45] C. di Valentin, G. Pacchioni, A. Selloni, S. Livraghi, and E. Giamello, "Characterization of paramagnetic species in N-doped TiO_2 powders by EPR spectroscopy and DFT calculations," *Journal of Physical Chemistry B*, vol. 109, no. 23, pp. 11414–11419, 2005.

[46] I. Nakamura, N. Negishi, S. Kutsuna, T. Ihara, S. Sugihara, and K. Takeuchi, "Role of oxygen vacancy in the plasma-treated TiO_2 photocatalyst with visible light activity for NO removal," *Journal of Molecular Catalysis A: Chemical*, vol. 161, no. 1-2, pp. 205–212, 2000.

[47] I. Justicia, P. Ordej, G. Canto et al., "Designed self-doped titanium oxide thin films for efficient visible-light photocatalysis," *Advanced Materials*, vol. 14, no. 19, pp. 1399–1402, 2002.